An Adaptive Optics System for Solid-State Laser Systems used in Inertial Confinement Fusion

J. T. Salmon, E. S. Bliss, J. L. Byrd, M. Feldman, M. A. Kartz,
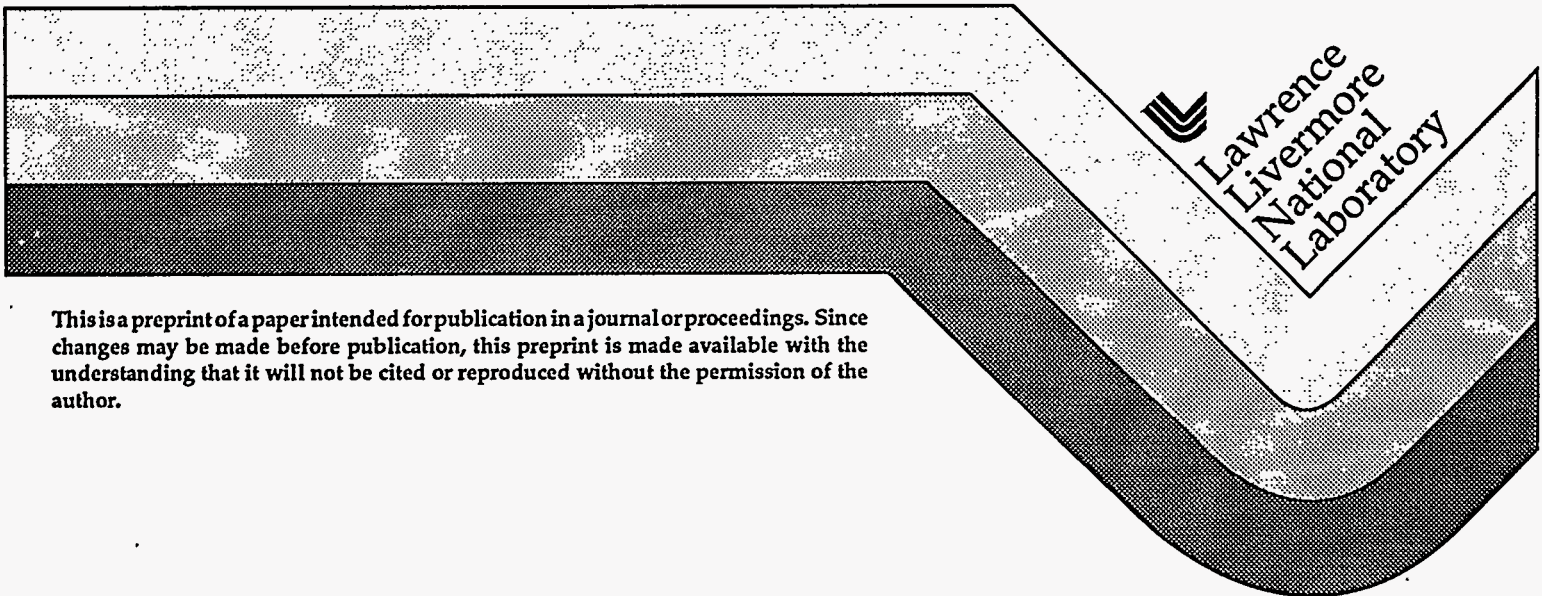J. S. Toeppen, B. VanWonterghem, and S. E. Winters

September 17, 1995

Lawrence Livermore National Laboratory

DISCLAIMER

DISCLAIMER

Portions of this document may be illegible in electronic image products. Images are produced from the best available original document.

An adaptive optics system for solid-state laser systems used in inertial confinement fusion[*]

J. T. Salmon, E. S. Bliss, J. L. Byrd, M. Feldman, M. A. Kartz,
J. S. Toeppen, B. VanWonterghem, and S. E. Winters

Lawrence Livermore National Laboratory
Livermore, CA 94551

ABSTRACT

Using adaptive optics we have obtained nearly diffraction-limited 5 kJ, 3 nsec output pulses at 1.053 μm from the Beamlet demonstration system for the National Ignition Facility (NIF). The peak Strehl ratio was improved from 0.009 to 0.50, as estimated from measured wavefront errors. We have also measured the relaxation of the thermally induced aberrations in the main beam line over a period of 4.5 hours. Peak-to-valley aberrations range from 6.8 waves at 1.053 μm within 30 minutes after a full system shot to 3.9 waves after 4.5 hours. The adaptive optics system must have enough range to correct accumulated thermal aberrations from several shots in addition to the immediate shot-induced error. Accumulated wavefront errors in the beam line will affect both the design of the adaptive optics system for NIF and the performance of that system.

Keywords: adaptive optics, deformable mirror, glass laser, inertial confinement fusion, laser, wavefront control

1. INTRODUCTION

The design for the National Ignition Facility (NIF) calls for 192 complex multipass amplifier chains, where each amplifier chain is fed by one of 4 master oscillators. Each amplifier chain includes regenerative amplifiers, multipass preamplifiers, and multipass power amplifiers and amplifies a pulse from about 1 nJ to 17 kJ. The effect of aberrations in these amplifiers are magnified by the number of times the beam passes through them. The largest contributors are the slabs in the multipass power amplifier, owing to the large pump power from the flashlamps and to the 4-passes through each slab inside it.

The net wavefront in NIF affects both the conversion efficiency of the frequency converters and the size of the focus spot on the target. Adaptive optics systems for high-power laser beams have been developed and are used at Lawrence Livermore National Laboratory.[1-4] A similar adaptive optics system was installed in the Beamlet demonstration facility to measure the amplitude and shape of both static and thermally induced aberrations in the beam at the frequency converters and to develop a method for correcting these aberrations during a full system shot.

2. SYSTEM DESCRIPTION

Beamlet is a large-scale multipass-amplifier laser chain that demonstrates concepts behind the NIF design. The beamlet system, shown schematically in Fig. 1, consists of (1) a front end, which includes the master oscillator, pulse shaping and frequency modulating electro-optical modules, and preamplifiers (regenerative and multipass), and (2) a main multipass amplifier and booster amplifier ahead of nonlinear crystals for harmonic frequency conversion. The adaptive optics components are also shown, with the deformable mirror and an input Hartmann sensor located between the front end and the main 4-pass amplifier. An output Hartmann sensor is located just before the harmonic frequency converters. Only one Hartmann sensor is used at a time to control the wavefront either at the input to the main multipass amplifier or at the frequency converters. The optical design of the diagnostic path includes an afocal telescope that relays a demagnified image of the deformable mirror to each

Hartmann sensor. Furthermore, afocal relay telescopes in the main beam line relay the plane of the deformable mirror to the approximate location of the primary source of aberrations, the amplifier in the main 4-pass cavity. This design minimizes distortion of the beam at the main amplifier arising from compensating aberrations introduced by the deformable mirror.
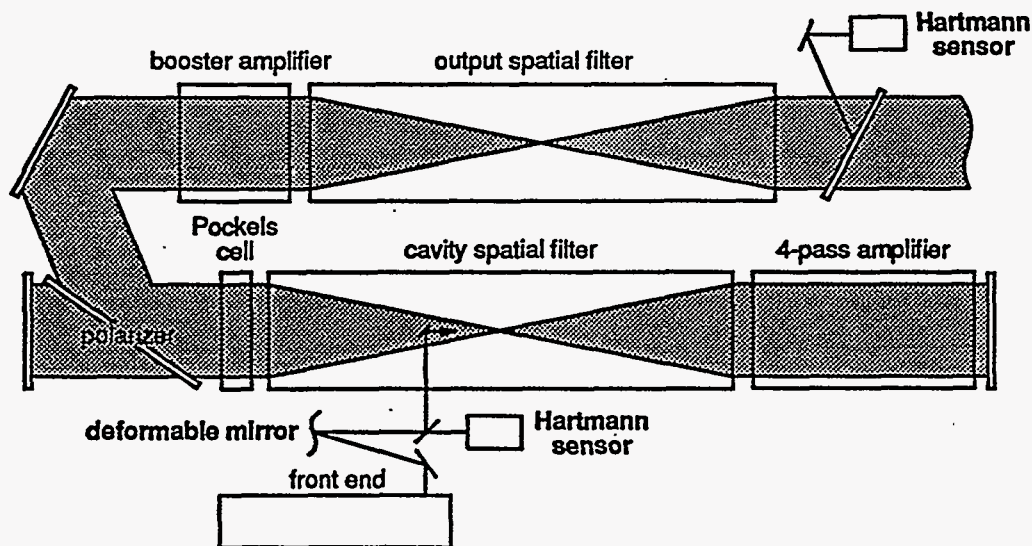

Fig. 1. The Beamlet laser chain with bold labels identifying adaptive optics components.

The adaptive optics system for Beamlet is designed to correct static aberrations in the main beam line and to precorrect dynamic aberrations induced in the main power amplifiers by absorption of pump light from the flashlamps. The accuracy of the controlled wavefront is achieved by calibrating each Hartmann sensor to an associated wavefront reference source.[5] The calibration of the sensor compensates for minor aberrations in the diagnostic path between the sampling optic in the main beam line and the lenslet array or the sensor. The output beam from the wavefront reference source is collimated to better than 1/5th wave peak-to-valley (p-v) over a 20 mm diameter at λ=1053 nm, as measured by a shear plate. The error in this measurement is primarily defocus. Since the Hartmann sensors in this system only measure the wavefront over a 5 mm diagonal and since the primary error in the wavefront reference source is defocus, the net error in the wavefront from the wavefront reference source is better than 1/10th wave p-v.

The deformable mirror, shown in Fig. 2, is 7 cm square and has 39 actuators forming equilateral triangular subapertures. The substrate is a continuous piece of Ultra-Low Expansion (ULE) glass with posts ground into the back side. The front side has a multilayer dielectric coating that is annealed to relieve stress-induced warping of the substrate. Electrostrictive actuators made of lead magnesium niobate (PMN) are attached to posts on the back of the substrate. When flattened, the assembled mirror has a residual surface figure that is flat to within 1/5th wave p-v and to within 1/30th wave rms at 1.053 μm, as measured by a phase-measuring interferometer at 633 nm. The influence function of the interior actuators is roughly Gaussian with a 1/e half-width that is about equal to the separation between actuators. The stroke of the actuators is sufficient to correct at least 5 waves p-v of astigmatism at 1.053 μm.

The adaptive optics Hartmann sensors, shown schematically in Fig. 3, use standard RS-170 monochrome video cameras and photolithographically produced arrays of 77 lenslets.[6] The focal ratio of each lenslet is 81.5 with a Fresnel number of 1.1. Hence, the size of each Hartmann spot in the focal plane is equal to half the distance between lenslet centers. The focal length is set by sandwiching index-matching fluid between the lenslet array and an optical flat. The CCD array is centered within the depth of focus of the lenslets, which minimizes the sensitivity of the centroids of the Hartmann spots to variations in the intensity distribution across each lenslet. A second video camera shows an image of the lenslets and is used with an insertable wire mask to set the alignment

of the Hartmann sensor to the deformable mirror, adjust the magnification of the diagnostic wavefront relay telescope, and image the plane of the deformable mirror to the lenslet array of the Hartmann sensors.

Fig. 2   Seven cm deformable mirror used in Beamlet system. The clear aperture is 6 cm square.

An additional (diagnostic) Hartmann sensor with 247 lenslets is adjacent to the output Hartmann sensor and provides an independent measurement of the wavefront at the frequency converters. This detector is also an RS-170 video camera, and the output image is captured and archived by an image analysis system. The archived images are post-processed to obtain the wavefront at 105 discrete points across the beam, as well as the peak-to-valley, root-mean-squared, and the sagitta of simple curvature in the principle axes of the wavefront in waves at 1053 nm. This independent diagnostic helps us determine system performance before, during, and after a system laser shot.

The controller electronics consist of three dedicated real-time processors housed in a VME chassis. The first processor analyzes the video image from a given adaptive optics Hartmann sensor and calculates the centroid of each Hartmann spot after applying a binary threshold (all pixels above the threshold are set to 1 and the rest set to 0). The second processor takes the centroids from the first processor, applies the control algorithm, and sends corrective signals to digital/analog (D/A) converters. The outputs from the D/A converters are amplified and applied to the actuators on the deformable mirror. The controller can put an arbitrary amount of defocus and astigmatism on the beam as specified by the user. The third processor runs an X-Windows user interface for interaction with the operator of the system. The processors communicate with each other through battery-backed shared memory.

3. SYSTEM OPERATION

The adaptive optics system can flatten the wavefront at the location of either Hartmann sensor and with either cw light or with pulsed light from a regenerative amplifier in the front end. The current closed-loop system bandwidth is about 3 Hz for cw light and about 1/50 Hz for regenerative amplifier light (limited by the 0.2 Hz pulse repetition frequency of the regenerative amplifier). The system can also prefigure the wavefront of the beam to the conjugate of a wavefront specified by the user. At this time the adaptive optics systems can prefigure the

deformable mirror only when operating with pulsed light from the regenerative amplifier. Furthermore, the system can capture an image of Hartmann spots during a main system shot, and that data can be used to improve the prefigure applied on subsequent shots.
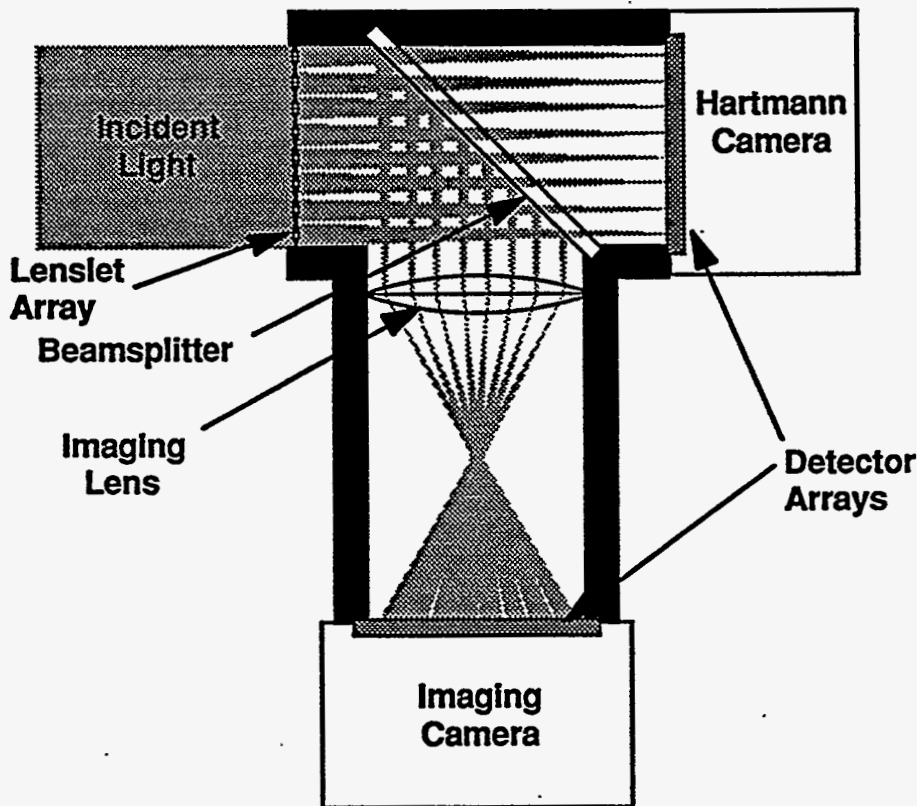

Fig. 3   Schematic of Hartmann sensor showing the two video cameras for data and alignment.

The procedure for compensating for thermally induced aberrations during a system shot is shown in Fig. 4. When initially setting the prefigure setpoint to "flat," the system can also introduce a set amount of defocus and astigmatism along the principal axes of the beam. The amount of focus and astigmatism initially introduced is based on previous experience with the Beamlet system. Once the setpoint is initially determined the adaptive optics loop is closed on the pulsed beam out of the regenerative amplifier. As stated above the closed-loop bandwidth is 1/50 Hz, which only compensates for static aberrations and thermally induced aberrations in solid media.

Shortly before the system shot the adaptive optics control loop is opened, and the frame grabber is armed for acquiring the image of Hartmann spots from the system shot. Once the image for the system shot is captured, the image is transferred to a second processor. The second processor calculates the displacement of the centroids from the desired positions of the Hartmann spots and determines the wavefront error induced by the shot. The prefigure setpoint is adjusted, and the control loop is closed again until shortly before the next shot.

The success of this procedure depends on the reproducibility of the thermally induced aberrations from shot to shot for a given pump energy and pulse power. Reproducibility is affected by (1) changes in stored and delivered charge

from the capacitors to the flashlamps, (2) changes in the illumination from the flashlamps both in amplitude and pattern, owing to loss or replacement of flashlamps, and (3) changes in the pulse power delivered by the preamplifiers in the front end of the multipass amplifier chain. Other factors include turbulence in the beam line that is driven by natural convection (buoyancy) in the main amplifiers. Since the amplifiers are sealed and are cooled by natural convection, turbulence induced aberrations become more important with each successive shot. The system cools back to equilibrium overnight.
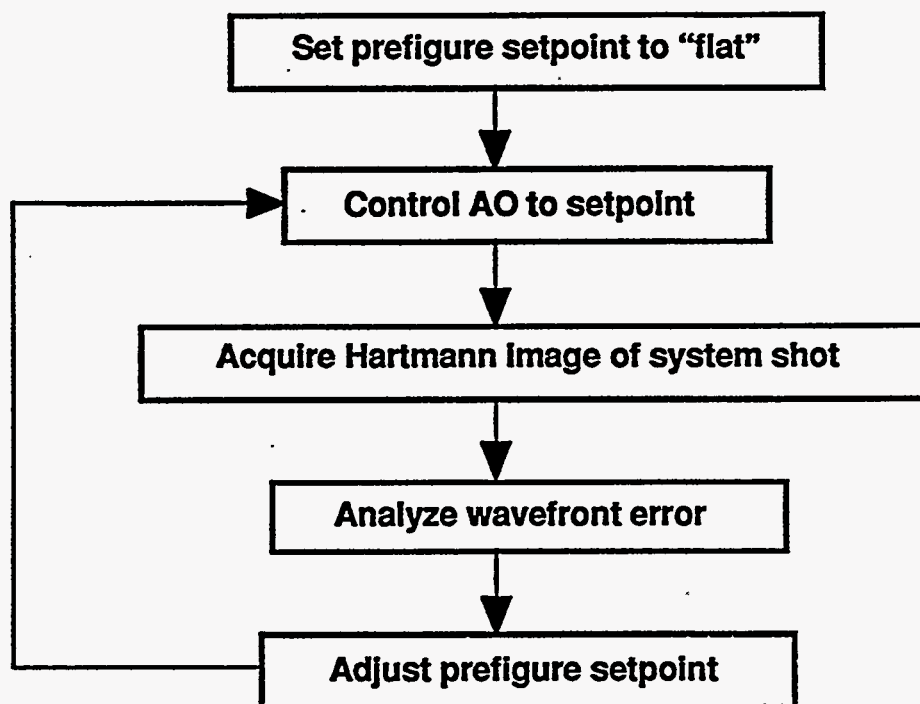

Fig. 4   Procedure for flattening the wavefront of a system shot by prefiguring the deformable mirror to compensate for a previous system shot.

4. RESULTS

Following the procedure outlined in Fig. 4 and based on previous experience with aberrations in the system, we set the initial "flat" with pure focus of 0.6 waves convergence and closed the adaptive optics control loop. Shortly before the shot we opened the control loop and acquired the shot image of Hartmann spots on both the adaptive optics Hartmann sensor and the diagnostics Hartmann sensor. Using the results from that shot, we altered the setpoint of the controller and drove the wavefront measured by the output adaptive optics Hartmann sensor to be conjugate to the one measured during the previous shot, relative to the initial focus of the beam. Shortly before the next shot we opened the loop and acquired the next shot on the Hartmann sensors.

The results of this exercise are shown in Fig. 5, where the "partially prefigured" wavefront is the one measured by the diagnostic Hartmann sensor during the first shot. The "uncorrected" wavefront is the "partially prefigured" wavefront with the 0.6 waves of focus added back numerically. The "fully prefigured" wavefront was measured with the diagnostic Hartmann sensor during the second shot. Note that the only numerically adjusted wavefront is the one marked "uncorrected". The pump light enters the left-front face and the right-rear face of each box. The uncorrected wavefront is primarily 2nd-order and 4th-order as predicted by Rotter et al.[7]

With precorrection we have reduced the total aberrations in Beamlet output pulses from 0.46 waves to 0.17 waves rms. From these wavefronts the estimated peak Strehl ratio increased from 0.009 to 0.50, more than a 50-fold improvement. The actual peak Strehl ratio is lower, since the diagnostic Hartmann sensor samples the wavefront

only 10 times across the beam width. Wavefront errors at higher spatial frequencies will not be detected, but will reduce the peak Strehl ratio. The wavefront correction includes compensation for static errors, slowly changing thermally induced errors, and dynamic pump-induced errors from the shots themselves.
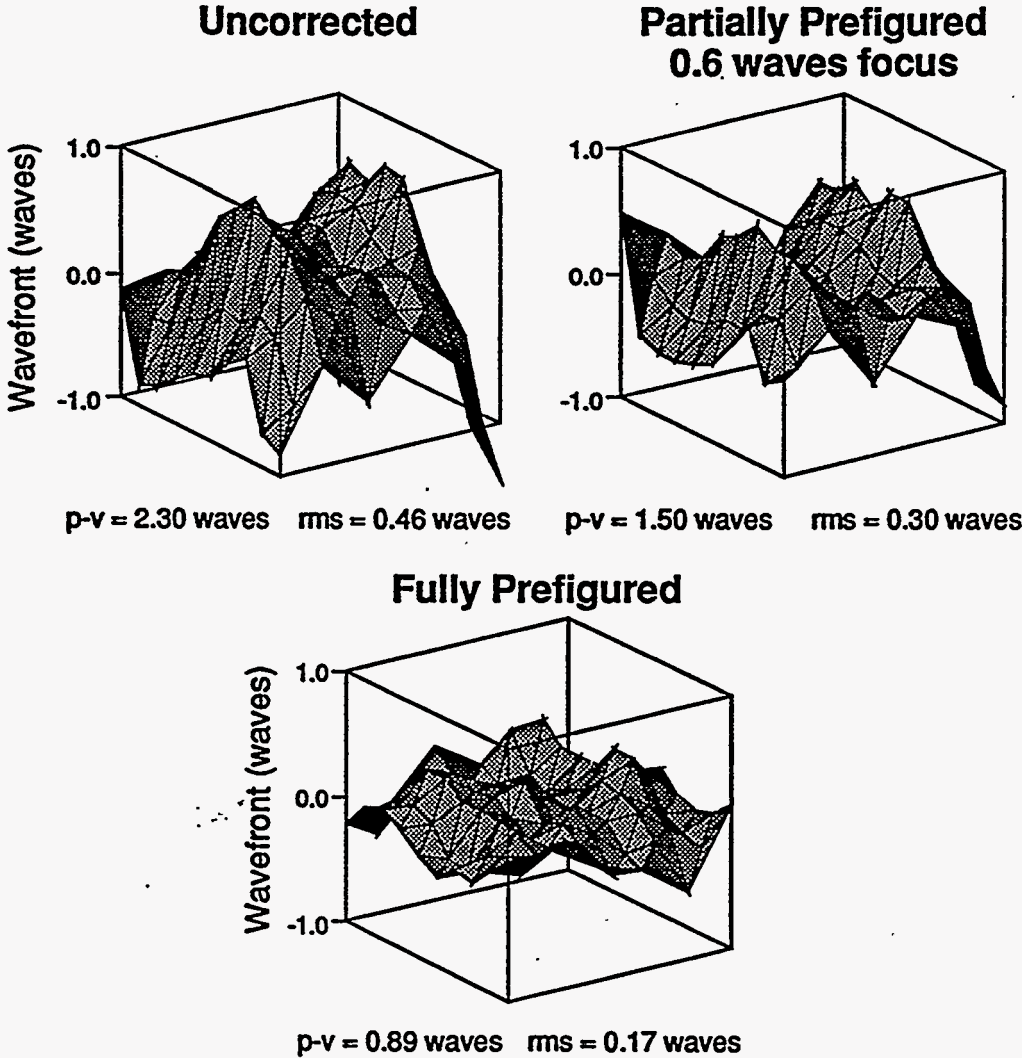

Fig. 5 Compensation of system shot in Beamlet by the adaptive optics system. Residual
wavefront error is dominated by turbulence in main beam path, which is not corrected.

Full compensation of the laser shot is limited by turbulence driven by buoyancy inside the main power amplifiers. These fluctuations are at temporal frequencies of a few Hertz, but include spatial frequencies higher than the capability of the current adaptive optics system. Operating with cw light and at a sampling rate of 30 Hz, the adaptive optics system can reduce the rms wavefront error owing to turbulence by about a factor of five. Even an improvement of a factor of two in the rms wavefront error would raise the Strehl ratio to 0.82, which would be essentially diffraction limited. To reach this limit we would need to operate with cw light instead of pulses from the regenerative amplifier, and we would need to automate the shot sequence to enable us to open the control loop 1 or 2 seconds before the next system shot.

We also measured the wavefront with the diagnostic Hartmann sensor at 30 minute intervals beginning 30 minutes after a shot and ending 4.5 hours after the shot. After the wavefront at the frequency converters was flattened immediately before the shot, the adaptive optics loop was not exercised during the 4.5 hour period. Since the PMN actuators are electrostrictive and have no creep, in contrast to PZT actuators which are piezoelectric, the

deformable mirror did not change shape during this test. From the measured wavefronts we determined the peak-to-valley error, the rms error, and the sagitta of the curvature across the principal axes of the beam (sagx and sagy). Note that the x-direction is parallel to the direction of the flashlamps and that positive sag represents convergence.

Figure 6 shows representative wavefronts from this set taken at 30, 90, and 240 minutes after the shot. As in Fig. 5, the pump light enters the left front and right rear sides of the boxes. Assuming that the initial thermally induced wavefront corresponds to the "uncorrected wavefront" in Fig. 5, the first half hour shows a growth in the amplitude of the wavefront and a reduction in the 4th-order component of the wavefront in the direction of the flashlamps, resulting in roughly a cylindrical shape. Between 30 minutes and 90 minutes the wavefront changes from a cylindrical shape to a saddle shape without much change in the overall peak-to-valley value. After 90 minutes the saddle shape remains nearly constant with only a reduction in the amplitude of the wavefront.

30 minutes   90 minutes

p-v = 6.80 waves   rms = 2.03 waves
sagx = -5.39 waves   sagy = 0.84 waves

p-v = 6.47 waves   rms = 1.69 waves
sagx = -3.31 waves   sagy = 3.35 waves

240 minutes

p-v = 4.71 waves   rms = 1.13 waves
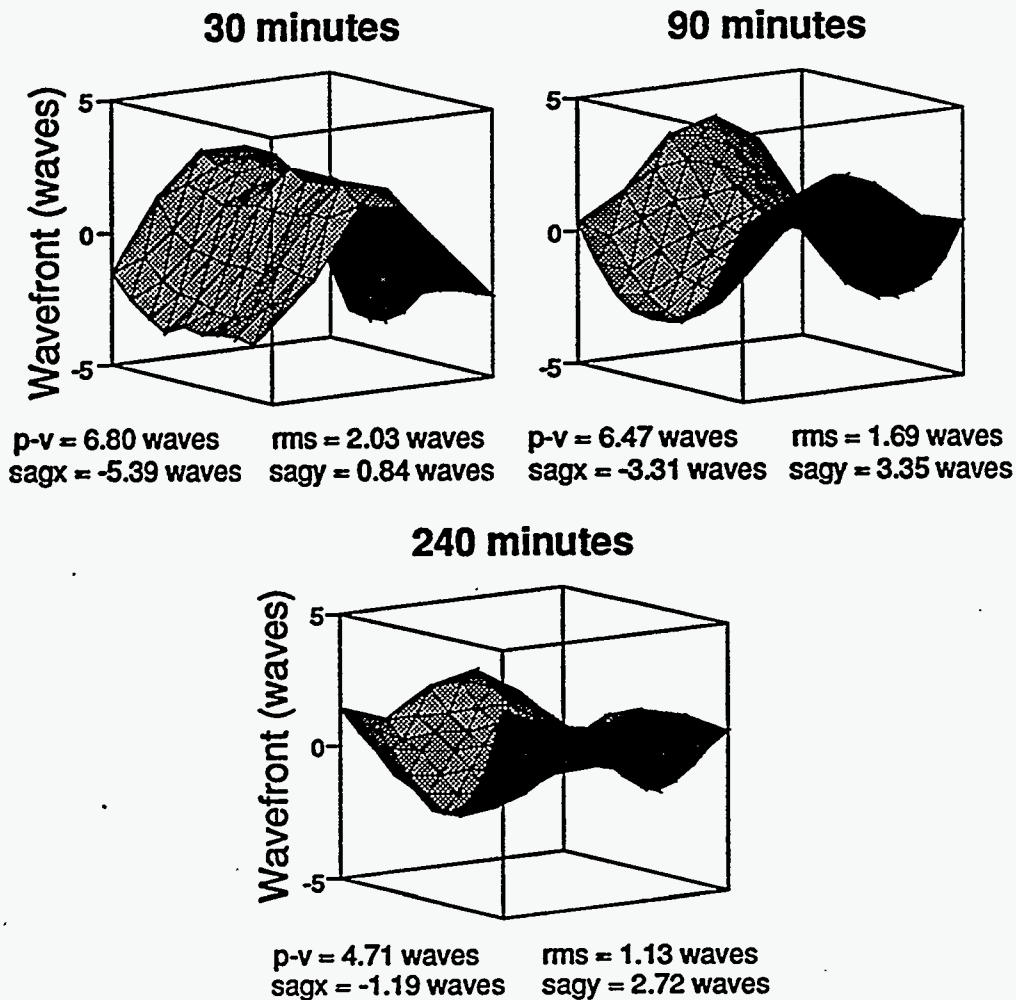sagx = -1.19 waves   sagy = 2.72 waves

Fig. 6   Decay of the thermally induced wavefront error in the Beamlet beam line at different times after a main system shot. The shape of the wavefront reaches steady state about 90 minutes after the shot and only changes amplitude after that.

Figure 7 shows the peak-to-valley, rms, sagx, and sagy plotted as a function of time after the shot. The growth in sagy while sagx shrinks monotonically corresponds to the transformation from primary cylinder to primary astigmatism. Note that over the 4.5 hours of the measurement the peak-to-valley of the wavefront only relaxed from about 6.8 waves to 3.9 waves. Furthermore, the thermally induced wavefront error introduced by a subsequent shot adds to the partially relaxed thermally induced wavefront error. Although the adaptive optics system can

compensate for wavefront errors exceeding 5 waves p-v, without active cooling of the amplifiers the range of the deformable mirror would be exceeded after only 2 shots within 4.5 hours or more.
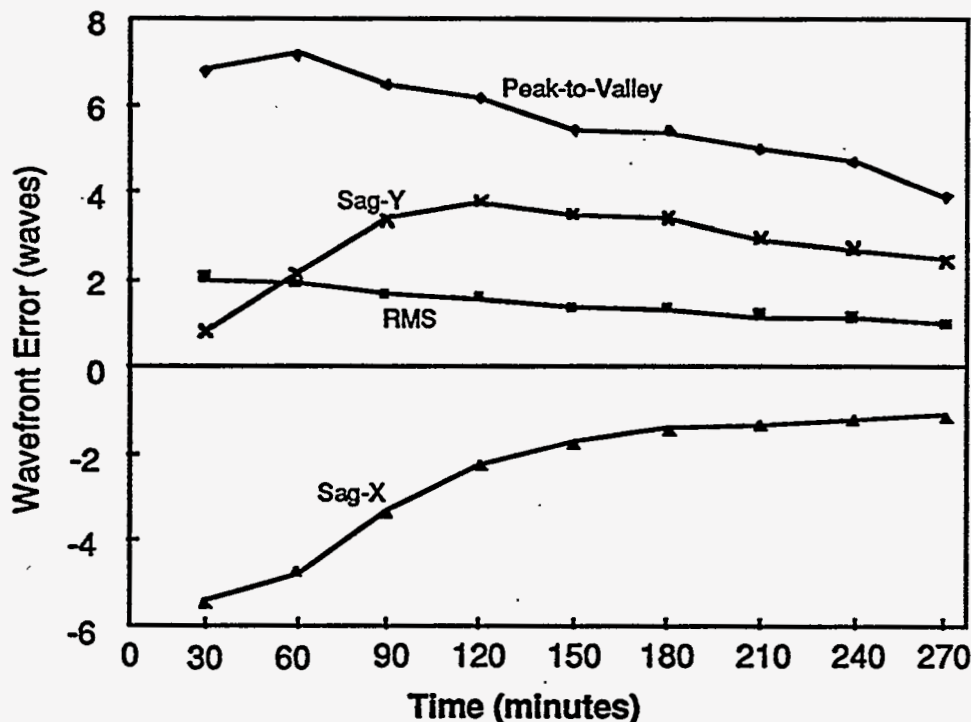

Fig. 7   History of relaxation of wavefront parameters in main beam line after a system shot.

5. IMPLICATIONS FOR NATIONAL IGNITION FACILITY

One reason for building the Beamlet demonstration facility is to learn about potential obstacles to the successful operation of the National Ignition Facility. The principal purpose of the adaptive optics system on Beamlet is to develop a method for compensating for aberrations in the beam during a system shot. We have found that prefiguring the deformable mirror to obtain the conjugate wavefront to the one measured on a previous shot of equal pump energy can correct the wavefront at least to the level of buoyancy-driven turbulent wavefront aberrations in the power amplifiers.

The performance of wavefront compensation in NIF will directly depend on (1) the reproducibility of the pump energy from shot to shot, (2) the magnitude of turbulence in the beam path, primarily in the power amplifiers where the beam is largest and the pump energy is the greatest, (3) the closed-loop bandwidth of the adaptive optics controller relative to the temporal power spectrum of turbulence in the beam line, (4) the time interval between opening the control loop for shot acquisition and the actual laser shot relative to the time scale of turbulence in the beam line, and (5) the spatial frequency bandwidth of the deformable mirror relative to the spatial power spectrum of the turbulence. Addressing these issues, future plans for beamlet include (1) using cw light instead of pulses from the regenerative amplifier for prefiguring for the next system shot, which will increase the closed-loop bandwidth from 0.02 Hz to 3 Hz and (2) reducing the time between opening the loop and the system shot. Increasing the spatial-frequency bandwidth of the deformable mirror would require a new deformable mirror with more actuators in the clear aperture. We will consider this option at a later date.

The required range of the deformable mirror depends on (1) the magnitude of aberrations, both static and thermally induced in the amplifiers with each system shot, (2) the rate of reduction of the thermally induced aberrations in the amplifiers, (3) the minimum elapsed time between shots specified by operations, and (4) the maximum number of shots in a day. An additional constraint to the system is the angular limit of the light that is

set by the size of the pinholes in the spatial filters that house the power amplifiers. The size of the pinholes will limit both the magnitude of the uncorrected wavefront of the beam in the system and the magnitude of the prefigured wavefront in the beam. Furthermore, the amplifiers in NIF will operate with the edge of the beam closer to the edge of the amplifier slabs than Beamlet, which will increase the aberration at the edges close to the flashlamps. Addressing both the pinhole throughput issue and the edge effects in the amplifiers in NIF, we will be deploying a deformable mirror as one of the cavity mirrors in the main multipass amplifier in Beamlet, where the beam will reflect twice. This location will double the net correction of the wavefront for a given displacement of the mirror surface, and it will distribute the prefiguring within the multipass amplifier, effectively reducing the maximum deviation of the wavefront from flat by roughly 50%. There is also a parallel effort in actively cooling the amplifiers after a system shot and an additional effort at reducing the magnitude of the thermally induced aberrations during a system shot.

The adaptive optics system in Beamlet has demonstrated near diffraction limited performance, achieving peak Strehl ratios of about 0.5, estimated from measurements of the wavefront error. Future activities should improve the performance of the system and demonstrate the utility of adaptive optics for NIF.

6. ACKNOWLEDGMENTS

7. REFERENCES

1. J.T. Salmon, J.W. Bergum, M.W. Kartz, R.W. Presta, and C.D. Swift, "Wavefront correction system based on an equilateral triangular arrangement of actuators," in *Active and Adaptive Optical Components and Systems II*, SPIE Proceedings 1920, 20 (1993).

2. J.T. Salmon, K. Avicola, J.M. Brase, J.W. Bergum, H.W. Friedman, C.T. Gavel, C.E. Max, S. D. Mostek, S.S. Olivier, R.W. Presta, R.J. Rinnert, C.W. Swift, K.E. Waltjen, C.L. Weinzapfel, and J.N. Wong, "An adaptive optics package designed for astronomical use with a laser guide star tuned to an absorption line of atomic sodium," in *Adaptive Optics in Astronomy*, SPIE Proceedings 2201, 212 (1994).

3. J.T. Salmon, J.W. Bergum, T.W. Long, E.L. Orham, R.W. Presta, C.D. Swift, R.A. Thomas, R.S. Ward, and C.L. Weinzapfel, "On-line closed-loop wavefront correction for a multikilowatt dye laser system," in *Technical Digest, Conference on Lasers and Electrooptics*, Optical Society of America, p. 402 (1992).

4. J.T. Salmon, E.S. Bliss, T.W. Long, E.L. Orham, R.W. Presta, C.D. Swift, and R.S. Ward, "Real-time wavefront correction system using a zonal deformable mirror and a Hartmann sensor," in *Active and Adaptive Optical Systems*, SPIE Proceedings 1542, 459 (1991).

5. M. Feldman, D.J. Mockler, R.E. English Jr, J.L. Byrd, and J.R. Salmon, "Self-referencing Mach-Zehnder interferometer as a laser system diagnostic," in *Active and Adaptive Optical Systems*, SPIE Proceedings 1542, 490 (1991).

6. J.S. Toeppen, E.S. Bliss, T.W. Long, and J.T. Salmon, "A video Hartmann wavefront diagnostic that incorporates a monolithic microlens array," in *Miniature and Micro-Optics: Fabrication and System Applications*, SPIE Proceedings 1544, 218 (1991).

7. M.Rotter, S. Doss, A. Erlandson, K. Jancaitis, G. LeTouzé, B. Van Wonterghem, and L. Zapata, "Optical performance modeling of large-aperture amplifiers for ICF," in *Conference on Laser Optics (LO'95)*, St. Petersburg, Russia, June 27-July 1, 1995, SPIE Proceedings, in press.